New Trans-Arctic shipping routes navigable by midcentury

Laurence C. Smith[1] and Scott R. Stephenson

Department of Geography, University of California, Los Angeles, CA 90095

Edited by Ellen S. Mosley-Thompson, Ohio State University, Columbus, OH, and approved January 25, 2013 (received for review August 21, 2012)

Recent historic observed lows in Arctic sea ice extent, together with climate model projections of additional ice reductions in the future, have fueled speculations of potential new trans-Arctic shipping routes linking the Atlantic and Pacific Oceans. However, numerical studies of how projected geophysical changes in sea ice will realistically impact ship navigation are lacking. To address this deficiency, we analyze seven climate model projections of sea ice properties, assuming two different climate change scenarios [representative concentration pathways (RCPs) 4.5 and 8.5] and two vessel classes, to assess future changes in peak season (September) Arctic shipping potential. By midcentury, changing sea ice conditions enable expanded September navigability for common open-water ships crossing the Arctic along the Northern Sea Route over the Russian Federation, robust new routes for moderately ice-strengthened (Polar Class 6) ships over the North Pole, and new routes through the Northwest Passage for both vessel classes. Although numerous other nonclimatic factors also limit Arctic shipping potential, these findings have important economic, strategic, environmental, and governance implications for the region.

climate change | human–environment | marine transportation modeling | Arctic maritime development | global change

Since 1979, satellite mapping has revealed an overall trend of decreasing late-summer sea ice extent in the Arctic, with the six lowest years on record occurring since 2006 (1). Climate model projections indicate that this overall trend will continue, leading to a seasonally ice-free (defined as <1 M km^2 in September) Arctic Ocean later this century (2–5). These projections have, in turn, fueled abundant discussion about possible new geographically shorter international shipping routes linking the Atlantic and Pacific Oceans by the Northern Sea Route or Northwest Passage (6–10). However, such suppositions remain highly speculative, because few studies have attempted to merge climate model output with numerical transportation analysis; thus, a quantitative assessment of how anticipated climate changes will calculably alter trans-Arctic navigation is lacking.

To address this deficiency, we applied the Arctic Transportation Accessibility Model (ATAM) (11) to individual and ensemble-averaged datasets of projected sea ice thickness and concentration from seven respected coupled atmosphere–ocean general circulation models (GCMs), assuming two different climate-forcing scenarios and vessel types at present (2006–2015) and by midcentury (2040–2059). The GCMs used were the Australian Community Climate and Earth-System Simulator versions 1.0 and 1.3 (ACCESS1.0, ACCESS1.3), the Geophysical Fluid Dynamics Laboratory version CM3 (GFDL-CM3), the Hadley Global Environment Model 2 Carbon Cycle (HadGEM2-CC), the Institut Pierre Simon Laplace medium resolution coupled ocean–atmosphere model (IPSL-CM5A-MR), the Max Planck Institute for Meteorology Earth System Model (MPI-ESM-MR), and the National Center for Atmospheric Research (NCAR) Community Climate System Model version 4 (CCSM4). Six of the GCMs (ACCESS1.0, ACCESS1.3, GFDL-CM3, HadGEM2-CC, IPSL-CM5A-MR, and MPI-ESM-MR) were selected by the Coupled Model Intercomparison Project, Phase 5 (CMIP5) for best reproducing observed total sea ice extent and volume over the period 1979–2010 (5). The seventh GCM (CCSM4) was selected owing to its realistic representation of Arctic sea ice interannual variability and radiation physics (4, 12).

To control for seasonality, simulations were restricted to the peak navigation month of September, when open water reaches its maximum annual extent. For each September of every year, the optimal least-cost navigation route, narrowly defined as the most temporally expedient navigation course minimizing total voyage travel time while also avoiding sea ice sufficiently thick and/or concentrated so as to obstruct a particular vessel class, was identified for hypothetical ships seeking to traverse the Arctic Ocean between the North Atlantic (Rotterdam, The Netherlands and St. John's, Newfoundland) and the Bering Strait (*Materials and Methods*). Note that the word optimal, as used here, refers simply to any technically feasible navigation route that most minimizes total transit time (i.e., through optimization of geographical distance with advantageous sea ice thickness and concentration conditions), with no consideration of economic, regulatory, jurisdictional, or other factors also important to transit time and/or route selection. All simulations were obtained in a Lambert Azimuthal Equidistant map projection such that routes using the shortest geographical distance between two points (great circle arcs) appear as straight lines in the final map products. Optimal navigation routes were determined for the Intergovernmental Panel on Climate Change (IPCC) representative concentration pathway (RCP) RCP 4.5 and RCP 8.5 climate-forcing scenarios, representing medium-low (+4.5 W/m^2) and high (+8.5 W/m^2) radiative forcing increases, respectively (13); and Polar Class 6 (PC6) and open-water (OW) vessels, with medium and no hull ice strengthening, respectively (14).

Results

Simulations of optimal navigation routes using ensemble-averaged, hind-casted (1979–2005) climate model outputs realistically mimic the geographically restricted late 20th century pattern of limited shipping activity in the Arctic, with transits for PC6 and OW vessels confined to the Northern Sea Route (Fig. 1). This pattern is largely replicated for current conditions (2006–2015), with only minor differences in shipping potential between the RCP 4.5 and 8.5 climate-forcing scenarios (Fig. 2 *A* and *C*). By midcentury (2040–2059), however, the region's overall navigation potential increases substantially (Fig. 2 *B* and *D*), with three conclusions broadly apparent across both climate-forcing scenarios as follows.

First, the feasibility for OW vessels to complete September trans-Arctic voyages along the Northern Sea Route (NSR) both increases in frequency and expands geographically, with numerous optimal September routes shifting northward away from the Russian Federation coast (Fig. 2 *B* and *D*, blue lines). During

Author contributions: L.C.S. designed research; S.R.S. performed research; L.C.S. and S.R.S. analyzed data; and L.C.S. and S.R.S. wrote the paper.

The authors declare no conflict of interest.

This article is a PNAS Direct Submission.

Freely available online through the PNAS open access option.

[1]To whom correspondence should be addressed. E-mail: lsmith@geog.ucla.edu.

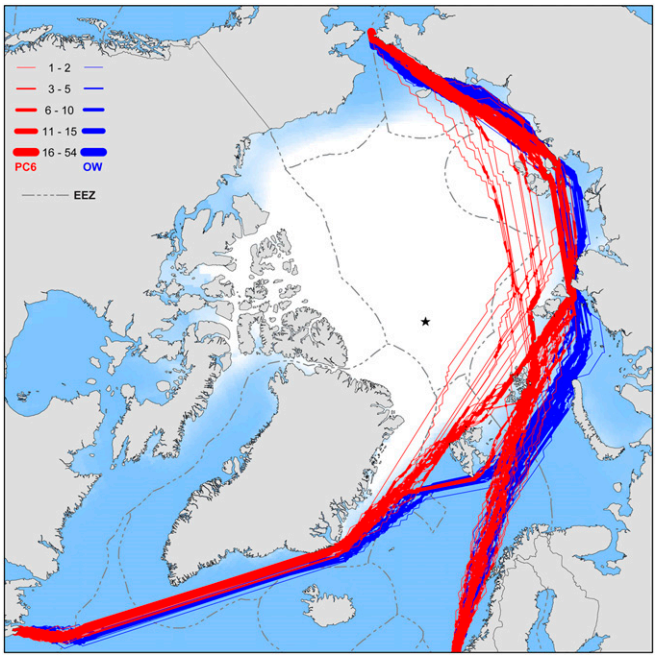

Fig. 1. ATAM-derived optimal September navigation routes for hypothetical ships seeking to cross the Arctic Ocean between the North Atlantic (Rotterdam, The Netherlands and St. John's, Newfoundland) and the Pacific (Bering Strait) during historical baseline conditions (consecutive years 1979–2005) as driven by ensemble-average GCM projections of sea ice concentration and thickness (ACCESS1.0, ACCESS1.3, GFDL-CM3, HadGEM2-CC, IPSL-CM5A-MR, MPI-ESM-MR, and CCSM4). Red lines indicate fastest available trans-Arctic routes for PC6 ships; blue lines indicate fastest available transits for common OW ships. Where overlap occurs, line weights indicate the number of successful transits using the same navigation route. Dashed lines indicate national 200-nm EEZ boundaries; white backdrop indicates period-average (1979–2005) sea ice concentration.

the 1979–2005 historical baseline period (Fig. 1), sea ice limited the probability of a technically feasible OW transit along the NSR to just ~40% in any given year, but this probability rises to 71%/61% for 2006–2015 and 94%/98% by 2040–2059 (for RCP 4.5/8.5, respectively). Although numerous other nonclimatic factors also limit the viability of Arctic marine shipping (15–17), from a purely geophysical sea ice perspective, the ability of unstrengthened OW ships to traverse the NSR and other areas of the eastern Arctic Ocean will increase.

Second, the emergence of unprecedented new optimal navigation routes for PC6 vessels through the central Arctic Ocean and Northwest Passage (NWP) is plainly evident by 2040–2059 (Fig. 2 *B* and *D*, red lines). This dramatic northward shift of optimal PC6 routes well away from the NSR (which dominates optimal PC6 traffic today) to the North Pole (for transits to/from Europe) and through the NWP (for transits to/from eastern North America) is apparent regardless of whether a +4.5 or +8.5 W/m^2 climate-forcing scenario is assumed. The emergence of a robust PC6 corridor directly over the North Pole, for example (Fig. 2 *B* and *D*), indicates that, in either scenario, sea ice will become sufficiently thin (e.g., <1.2-m thick at 100% ice concentration) and/or diffuse such that a critical technical threshold is surpassed, and the shortest great circle route thus becomes feasible, for ships with moderate ice-breaking capability.

Third, the Northwest Passage (NWP), arguably the most historically famed of potential shipping routes through the Arctic, has the lowest navigation potential both historically and at present but opens substantially by 2040–2059. Under no simulations do ice conditions in the NWP attract transits to/from Europe for either vessel class (Fig. 2, all lines). However, for transits to/from eastern North America, the NWP is more efficacious than any other route 100% of the time for PC6 vessels (for either climate-forcing scenario), and is often more efficacious than the NSR for OW vessels by midcentury. During the 1979–2005 historical baseline period (Fig. 1), sea ice limited the probability of a feasible OW transit through the NWP to just ~15% in any given year, but this probability increases to 17%/27% by 2006–2015 and 53%/60% by 2040–2059 (for RCP 4.5/8.5, respectively). Put simply, by midcentury, September sea ice conditions have changed sufficiently in the NWP such that trans-Arctic shipping to/from North America can commonly capitalize on the ~30% geographic distance savings that this route offers over the NSR.

Discussion

This analysis presents simulations of changing technical feasibility of trans-Arctic ship navigation as influenced by climate-induced changes in sea ice concentration and thickness. Its core findings of rising optimal OW navigability along the NSR, newly optimal PC6 navigability through the central Arctic Ocean and NWP, and newly optimal OW navigability through the NWP are evident in both climate-forcing scenarios examined (RCP 4.5 and RCP 8.5, corresponding to +4.5 and +8.5 W/m^2 increases in radiative forcing, respectively), and because current climate models often lag behind real-world satellite observations of shrinking Arctic sea ice cover, they may well be conservative. Additional refinements to these optimal route simulations are anticipated as the available suite of coupled atmosphere–ocean general circulation models continues to incorporate improved representation of sea ice geophysics and additional processes, particularly ice ridging and decay, that are also impactful to shipping. We reiterate that these results reflect conditions for peak late-summer (September) shipping season only, and are driven solely by projected reductions in sea ice thickness and concentration. Although sea ice currently represents the single greatest obstacle to trans-Arctic shipping, numerous additional factors, including dearth of services and infrastructure, high insurance and escort fees, unknown competitive response of the Suez and Panama Canals, poor charts, and other socioeconomic considerations, remain significant impediments to maritime activity in the region (15–17).

Such factors permitting, our findings have important implications for trade, environmental risk, and evolving strategic and governance policies in the Arctic. The prospect of common OW ships (which comprise the vast majority of the global fleet) entering the Arctic Ocean in late summer, and even its remote central basin by moderately ice-strengthened vessels (as are used today in the Baltic), heightens the urgency for a mandatory International Maritime Organization (IMO) regulatory framework to ensure adequate environmental protections, vessel safety standards, and search-and-rescue capability for this unique and challenging polar ecosystem (18). The new "Supra-Polar" routes identified here can deviate outside of the standard 200-nm Exclusive Economic Zone (EEZ) of the Russian Federation, thus enhancing the potential appeal of the international high seas and Norwegian, Greenlandic, Canadian, and US (assuming eventual US ratification of the United Nations Convention on the Law of the Sea) EEZs (Fig. 2, dashed lines) for transit relative to the NSR (where the Russian Federation currently charges escort fees to international vessels) (16). Finally, two chronic, long-standing debates over the status of international shipping through the NWP (19, 20) and US ratification of the United Nations Convention on the Law of the Sea (21) may warrant renewed attention, in light of its nascent navigability and the broader circumpolar changes projected here.

Materials and Methods

Sea ice parameters were obtained from monthly ice concentration and thickness time series from the ACCESS1.0, ACCESS1.3, GFDL-CM3, HadGEM2-CC, IPSL-CM5A-MR, MPI-ESM-MR, and CCSM4 GCMs (22, 23). Of these GCMs,

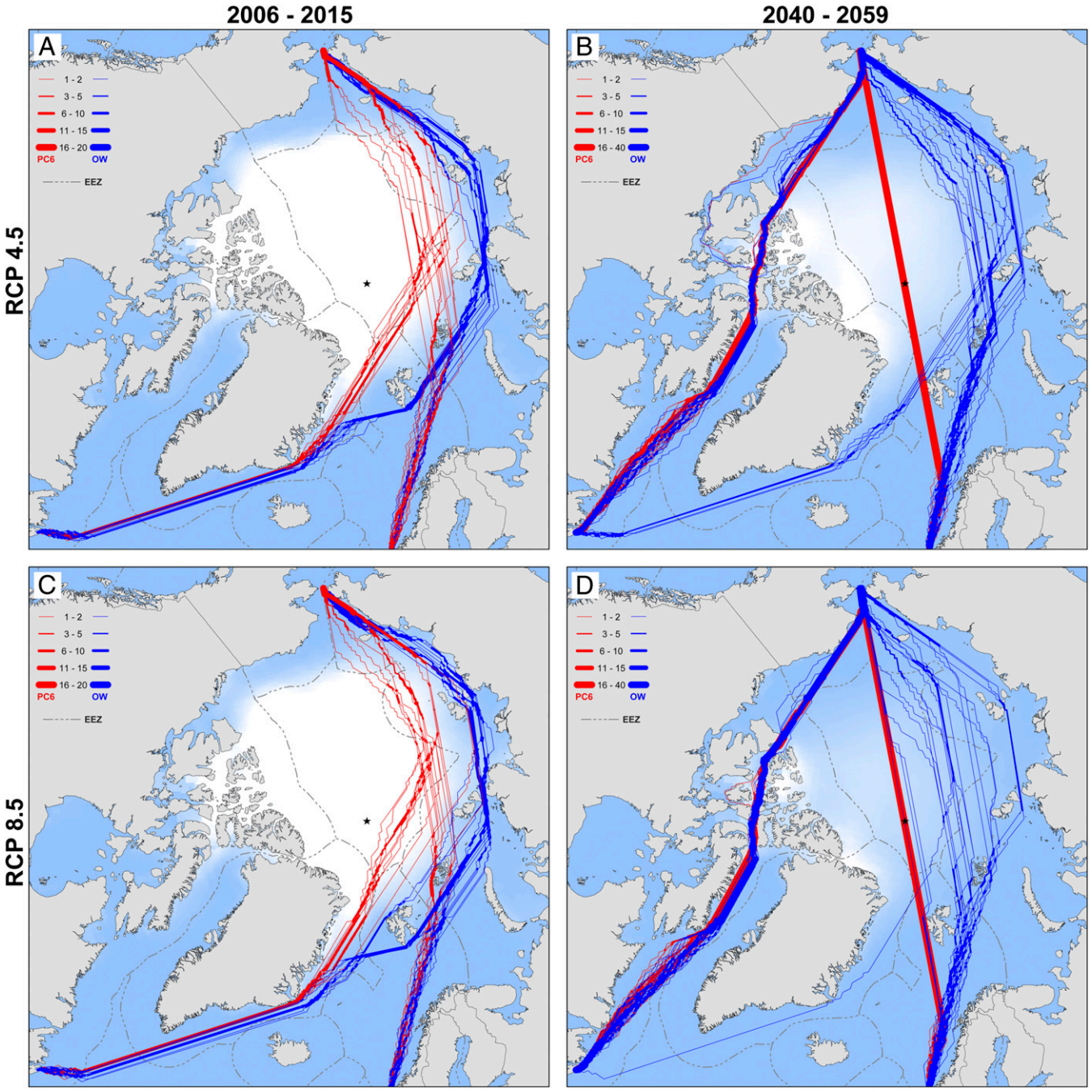

Fig. 2. ATAM-derived optimal September navigation routes for hypothetical ships seeking to cross the Arctic Ocean between the North Atlantic (Rotterdam, The Netherlands and St. John's, Newfoundland) and the Pacific (Bering Strait) during consecutive years 2006–2015 (*A* and *C*) and 2040–2059 (*B* and *D*) as driven by ensemble-average GCM projections of sea ice concentration and thickness assuming RCPs 4.5 (*A* and *B*; medium-low radiative forcing) and 8.5 (*C* and *D*; high radiative forcing) climate change scenarios. Red lines indicate fastest available trans-Arctic routes for PC6 ships; blue lines indicate fastest available transits for common OW ships. Where overlap occurs, line weights indicate the number of successful transits using the same navigation route. Dashed lines indicate national 200-nm EEZ boundaries; white backdrops indicate period-average sea ice concentrations in 2006–2015 (*A* and *C*) and 2040–2059 (*B* and *D*).

CCSM4 is most conservative (i.e., most overestimates ice extent) owing to its weaker Arctic climate response than other models, including an ~16% reduced Arctic amplification relative to CCSM3 (4). Individual and ensemble-averaged GCM runs were used for two end-member climate change scenarios, RCP 4.5 (with a medium-low radiative forcing of +4.5 W/m^2) and RCP 8.5 (with a high radiative forcing of +8.5 W/m^2) (13), for the two study periods encompassing present (2006–2015) and midcentury (2040–2059) conditions. Individual and ensemble-average hind-casted GCM model outputs (with no climate forcing) were also studied for the historical baseline period (1979–2005). For each of these seven climate models, three study periods, and two climate-forcing scenarios (for 2006–2015 and 2040–2059 only), individual time series of monthly mean September sea ice concentrations and thicknesses were obtained for each GCM and projected to a Lambert Azimuthal Equidistant projection centered on the Bering Strait (65°38′36″ N, 169° 11′42″ W) at 20 km^2 resolution using nearest-neighbor interpolation. These time series were also averaged to produce seven-model ensemble datasets of sea ice thickness and concentration to produce Figs. 1 and 2.

Least-cost navigation routes were derived from the described individual and ensemble-average datasets in ATAM (11, 24) modified as follows. To comply with standard maritime convention, GCM model output was adap-

ted for use in the Canadian Arctic Ice Regime Shipping System (AIRSS), a widely used maritime framework used to assess navigation safety in a given ice regime as a function of ice conditions and the structural and engineering capabilities of a particular vessel class (25). Under AIRSS, the ability of a ship to safely navigate ice-covered waters is given by the ice numeral (*IN*):

$$IN = (C_a * IM_a) + (C_b * IM_b) + \ldots + (C_n * IM_n),$$

where C_a is the concentration in tenths of ice type *a*, IM_a is the ice multiplier of ice type *a*, C_b is the concentration in tenths of ice type *b*, and so on. Ice type describes the physical properties of ice and is closely related to ice age, because older ice tends to be thicker and stronger than younger ice owing to annual accretion of ice layers and reduced brine inclusions, thus posing greater hazard to ships (26). *IM*s, which are based on ice type and vessel class, are a series of nonzero integers ranging from −4 to 2, with higher values denoting lower risk. A negative *IM* signifies that the ice regime presents significant hazard and should be avoided. Pressure ridging and decay effects were not considered, because these processes are not explicitly modeled by today's current suite of available GCMs.

GCM outputs of sea ice concentration were input directly to the AIRSS *IN* framework. GCM outputs of ice thickness were categorized into *IM* values by estimating ice type from thickness ranges, using either standard AIRSS guidelines (for ice thicknesses ranging from 0 to 120 cm) (25) or an empirical regression model based on analysis of remotely sensed data (for ice thicknesses > 120 cm) (11). To span a range of capital investment in ship capability, simulations were run for a moderately ice-strengthened PC6 vessel (capable of summer/autumn operation in medium first-year ice, which may include old ice inclusions; assumed here as capable of breaking up to 120 cm of ice thickness in continuous 100% concentrated ice) and a common OW vessel (no ice strengthening; assumed here as capable of breaking up to 15 cm of ice thickness in continuous 100% concentrated ice). The AIRSS framework identifies six ice types (plus one OW type) with associated thickness ranges as follows: gray (10–15 cm), gray-white (15–30 cm), thin first-year first stage (30–50 cm), thin first-year second stage (50–70 cm), medium first year (70–120 cm), and thick first year (first-year ice over 120 cm) (25). Ice with thickness greater than 0 and less than 10 cm was aggregated with gray ice. Although this approach does not account for possible thickness variations within age classes or within ice of uniform age owing to seasonal melt–freeze cycles, it is generally true that age and thickness are well correlated at a given time of year (27, 28). Note that AIRSS distinguishes vessel ice capability by type (categories A–E) for operational use in Canada (25). The IMO Polar Class system, in contrast, was developed to harmonize construction and operating standards throughout the Arctic region (14). In accordance with international adoption of Polar Class nomenclature, this study follows the maritime convention that the AIRSS type A class is nominally equivalent to IMO PC6 (14, 25). The AIRSS type E category includes vessels intended for ice-free navigation only, and it is here referred to as OW.

Thickness ranges for older ice classes (i.e., second year and multiyear ice that has survived one and two or more melt seasons, respectively) were estimated from empirical observations relating ice age to thickness. Maslanik et al. (29) calculate median February/March proxy ice thicknesses for yearly age classes from 2004 to 2008 by combining ICESat freeboard ice-thickness measurements (30) with ice age grids derived from Lagrangian drift tracking. This methodology was repeated using October/November ICESat data from 2003 to 2007 to obtain proxy thicknesses for second-year and multiyear ice at the beginning of the freeze cycle. Weekly ice age grids were obtained from Maslanik et al. (29) for the period 2003–2007, and grids from week 41 to 48 of each year were averaged to obtain October/November mean ice age. Ice thickness and age grids were then overlaid in the ArcGIS geographic information system (GIS), and the median thickness value spatially coincident with each age class was averaged over the period 2003–2007, providing an October/November counterpart to the February/March estimates by Maslanik et al. (29). The September age–thickness relationship was then interpolated from a linear regression model between February/March and October/November thickness values (representing maximum and minimum annual thickness, respectively). By this method, multiyear ice was thus defined where September thickness exceeds 189 cm, second-year ice was defined where September thickness ranges from 151 to 189 cm, and thick first-year ice was defined where September thickness ranges from 120 to 151 cm.

In sum, the described procedures allow *IM* values for PC6 (IM_{PC6}) and OW (IM_{OW}) vessel classes to be derived from GCM outputs of ice thickness (T; in centimeters) as follows:

$$IM_{PC6} = \begin{cases} 2, \text{if } 0 \le T < 70, \\ 1, \text{if } 70 \le T < 120, \\ -1, \text{if } 120 \le T < 151, \text{and} \\ -3, \text{if } 151 \le T < 189, \\ -4, \text{if } T \ge 189 \end{cases}$$

$$IM_{OW} = \begin{cases} 2, \text{if } T = 0, \\ 1, \text{if } 0 < T < 15, \\ -1, \text{if } 15 \le T < 70, \\ -2, \text{if } 70 \le T < 120, \\ -3, \text{if } 120 \le T < 151, \\ -4, \text{if } T \ge 151 \end{cases}$$

Optimal navigation routes were computed using a least-cost path algorithm as follows. Using the *IM* values obtained above, *IN* rasters for PC6 and OW vessels were created for each September of every year for all study periods (1979–2005, 2006–2015, and 2040–2059), two climate-forcing scenarios (RCPs 4.5 and 8.5), and two vessel classes (PC6 and OW). Navigation simulations were performed for both individual GCM runs and seven-model ensemble averages. Raster cells identified as having a negative *IN* for a given ship class were reclassified as inaccessible. Ship travel times (minutes per kilometer) were computed for all remaining areas using published *IN*–vessel speed relationships as published by McCallum (31). Next, each resultant September travel time raster was converted in GIS to a vector mesh of uniformly spaced nodes (20-km posting), with each node linked by eight line segments to its eight immediately adjacent neighbors (four orthogonal and four diagonal), and each line segment was coded with the travel time required to traverse the segment. Each mesh was then treated as a network surface in GIS, and the optimal, least-cost path was computed as the route accumulating the lowest possible travel time between origin and destination. Routes originated to/from two North Atlantic ports (Rotterdam, The Netherlands and St. Johns, Newfoundland) and terminated at the Bering Strait. For any year in which no trans-Arctic voyage was possible owing to ice obstruction equal to or exceeding the vessel class limit, no least-cost route was computed. Transit success rates were computed as the percentage of years in which a September transit was possible across all individual GCM model runs for all Septembers contained within the study period. Final summary map products were generated from ensemble-averaged sea ice thickness and concentration datasets, with line widths of the plotted navigation routes (blue, OW; red, PC6) proportional to frequency of use, and underlain by period-average September sea ice concentration.

ACKNOWLEDGMENTS. Constructive, helpful reviews by two anonymous readers are gratefully acknowledged. Matt Zebrowski of the University of California, Los Angeles Department of Geography provided graphic art assistance with Figs. 1 and 2. This work was supported by the National Science Foundation and the National Aeronautics and Space Administration (NASA) Cryosphere Program.

1. NSIDC (2012) *National Snow & Ice Data Center Ongoing Data Updates*. Available at www.nsidc.org. Accessed December 20, 2012.
2. Holland MM, Bitz CM, Tremblay B (2006) Future abrupt reductions in the summer Arctic sea ice. *Geophys Res Lett* 33:L23503, 10.1029/2006GL028024.
3. Wang M, Overland JE (2009) A sea ice free summer Arctic within 30 years? *Geophys Res Lett* 36:L07502, 10.1029/2009GL037820.
4. Vavrus SJ, Holland MM, Jahn A, Bailey DA, Blazey BA (2012) Twenty-first-century arctic climate change in CCSM4. *J Clim* 25(8):2696–2710, 10.1175/JCLI-D-11-00220.1.
5. Massonnet F, et al. (2012) Constraining projections of summer Arctic sea ice. *The Cryosphere Discuss* 6:2931–2959, 10.5194/tcd-6-2931-2012.
6. Cressey D (2011) Scientific challenges in the Arctic: Open water. *Nature* 478(7368): 174–177, 10.1038/478174a.
7. Lasserre F, Pelletier S (2011) Polar super seaways? Maritime transport in the Arctic: An analysis of shipowners' intentions. *J Transp Geogr* 19(6):1465–1473, 10.1016/j.jtrangeo.2011.08.006.
8. Schoyen H, Brathen S (2011) The Northern Sea Route versus the Suez Canal: Cases from bulk shipping. *J Transp Geogr* 19(4):977–983, 10.1016/j.jtrangeo.2011.03.003.
9. Blunden M (2012) Geopolitics and the Northern Sea Route. *Int Aff* 88(1):115–129, 10.1111/j.1468-2346.2012.01060.x.
10. Astill J (June 16, 2012) The melting north (special report: The Arctic). *The Economist*. Available at www.economist.com/node/21556798.
11. Stephenson SR, Smith LC, Agnew JA (2011) Divergent long-term trajectories of human access to the Arctic. *Nat Clim Chang* 1:156–160, 10.1038/nclimate1120.
12. Holland MM, et al. (2012) Improved sea ice shortwave radiation physics in CCSM4: The impact of melt ponds and aerosols on Arctic sea ice. *J Clim* 25(5):1413–1430, 10.1175/JCLI-D-11-00078.1.

13. van Vuuren DP, et al. (2011) The representative concentration pathways: An overview. *Clim Change* 109:5–31, 10.1007/s10584-011-0148-z.
14. International Maritime Organization (IMO) (2002) *Guidelines for Ships Operating in Arctic Ice-Covered Waters*, MSC/Circ.1056-MEPC/Circ.394 (International Maritime Organization, London).
15. AMSA (2009) *Arctic Marine Shipping Assessment 2009 Report* (Arctic Council), pp 1–88.
16. Liu M, Kronbak J (2010) The potential economic viability of using the Northern Sea Route (NSR) as an alternative route between Asia and Europe. *J Transp Geogr* 18(3):434–444, 10.1016/j.jtrangeo.2009.08.004.
17. Brigham LW (2010) Think again: The Arctic. *Foreign Policy* 72:70–74.
18. Brigham L (2011) Marine protection in the Arctic cannot wait. *Nature* 478(7368):157, 10.1038/478157a.
19. Gerhardt H, Steinberg PE, Tasch J, Fabiano SJ, Shields R (2010) Contested sovereignty in a changing Arctic. *Ann Assoc Am Geogr* 100(4):992–1002, 10.1080/00045608.2010.500560.
20. Elliot-Meisel E (2009) Politics, pride, and precedent: The United States and Canada in the northwest passage. *Ocean Dev Int Law* 40(2):204–232, 10.1080/00908320902864813.
21. Allen TH, Armitage RL, Hamre JJ (April 25, 2011) Odd man out at sea. *The New York Times*, Section A, p 25.
22. World Climate Research Programme (2012) *Coupled Model Intercomparison Project Phase 5 Data Archive*. Available at http://cmip-pcmdi.llnl.gov/index.html. Accessed November 15, 2012.
23. Gent PR, et al. (2011) The Community Climate System Model Version 4. *J Clim* 24(19):4973–4991, 10.1175/2011JCLI4083.1.
24. Stephenson RR, Smith LC, Brigham LW, Agnew JA (2013) Projected 21st-century changes to Arctic marine access. *Climatic Change*, 10.1007/s10584-012-0685-0.
25. Transport Canada (1998) *Arctic Ice Regime Shipping System (AIRSS) Standards (Ottawa)* (Transport Canada, Ottawa).
26. Johnston ME, Timco GW (2008) *Understanding and Identifying Old Ice in Summer*, Technical Report CHC-TR-055, National Research Council Canada, Canadian Hydraulics Centre (Ottawa) (Transport Canada, Ottawa).
27. Fowler C, Emery WJ, Maslanik JA (2004) Satellite-derived evolution of Arctic sea ice age: October 1978 to March 2003. *IEEE Trans Geosci Remote Sens* 1(2):71–74, 10.1109/LGRS.2004.824741.
28. Hunke EC, Bitz CM (2009) Age characteristics in a multidecadal Arctic simulation. *J Geophys Res* 114:C08013, 10.1029/2008JC005186.
29. Maslanik JA, et al. (2007) A younger, thinner Arctic ice cover: Increased potential for rapid, extensive sea-ice loss. *Geophys Res Lett* 34:L24501, 10.1029/2007GL032043.
30. Kwok R, Cunningham GF, Zwally HJ, Yi D (2007) Ice, cloud, and land elevation satellite (ICESat) over Arctic sea ice: Retrieval of freeboard. *J Geophys Res* 112:C12013, 10.1029/2006JC003978.
31. McCallum J (1996) *Safe Speed in Ice: An Analysis of Transit Speed and Ice Decision Numerals. Ship Safety Northern (AMNS)* (Transport Canada, Ottawa).